Asian Journal of Chemistry; Vol. 34, No. 10 (2022), 2551-2560

ASIAN JOURNAL OF CHEMISTRY

https://doi.org/10.14233/ajchem.2022.23758

Synthesis, Spectroscopic Analysis, Antimicrobial and Antioxidant Screening of Some Organyltellurium(IV) Complexes

MAHAK DALAL, NIDHI ANTIL, K.K. VERMA and SAPANA GARG*

Department of Chemistry, Maharshi Dayanand University, Rohtak-124001, India

*Corresponding author: E-mail: sapanagarg1511@gmail.com

Received: 2 February 2022; *Accepted*: 14 April 2022; *Published online*: 19 September 2022; AJC-20955

In present study, six new organyltellurium(IV) Schiff base complexes with the formula $RTeCl_2$·H4AP (**1a-c**) and R_2TeCl·H4AP (**1d-f**), where R= 4-methoxyphenyl, 4-hydroxyphenyl and 3-methyl-4-hydroxyphenyl, ligand H4AP = 1-(((4-hydroxyphenyl)imino)methyl)-naphthalen-2-ol obtained from the condensation of 2-hydroxy-1-naphthaldehyde with 4-aminophenol were synthesized and characterized by elemental analysis, molar conductance, mass spectrometry, FT-IR, UV-visible, ^{1}H NMR, ^{13}C NMR spectroscopy. Correlation of all spectroscopic data suggested that Schiff base ligand (H4AP) acts as bidentate (ON) ligand coordinated to tellurium ion *via* naphthalene ring-O and imine-N with the distorted square pyramidal geometry around the tellurium ion. DFT based calculations were done for the ligand and its metal complexes to confirm the geometry of complexes. Chemical quantum parameters were determined for the ligand and the complexes. The antioxidant activity of the Schiff base and their organyltellurium(IV) complexes were assessed on the basis of radical scavenging effect of DPPH. The free Schiff base and its complexes were screened for the *in vitro* antifungal and antibacterial activity. The results show that the organyltellurium(IV) complexes were more active than the Schiff base. The molecular docking simulations carried out to study the probable binding modes of the ligand with various proteins receptors such as *C. albicans* and *E. coli*.

Keywords: 2-Hydroxy-1-naphthaldehyde, 4-Aminophenol, Antibacterial activity, Antifungal activity, Antioxidant activity.

INTRODUCTION

Schiff bases are among the most versatile families of organic ligands, which can form coordinate compounds with various metal ions in different oxidation states. The excellent chelating and donor abilities are due to basicity of lone pair of sp^2 hybrid nitrogen atom of imine (-CH=N-) linkage and of other donor atom present near to the imine group. Schiff bases are structurally diverse [1] and are called organic bioactive ligands [2] as they show broad biological activities such as antimalarial [3], anticonvulsant [4], antioxidant [5-8], antifungal [9], antibacterial [10-12], anti-influenza A virus [13], antitubercular [14] and so forth. They are also widely studied for their applications in catalysis, bioorganic, organic syntheses, separation processes, metallic deactivator and industrial purposes.

Naphthaldehyde Schiff bases with hydroxyl substituent at *ortho*-position possess some interesting properties such as thermochromism and photochromism [15] in the solid state, making the Schiff bases useful for the measurement and control of radiation intensity in optical computers and other display systems. On the other hand, the Schiff base derived from substituted naphthaldehyde are known to behave as the most potent antimicrobial agent [16,17], organic semiconductors [18], electrochemical sensor [19] and show significant cytotoxicity activity [20-25] against cancerous cells. Different organyltellurium(IV) chlorides are well known for their electron accepting nature *i.e.* behaving as Lewis acids and were reported to form stable complexes with Schiff bases having N, O and S donor atoms. As far as biological activity is concerned, the organyltellurium(IV) compounds such as organyltelluranes and organyltellurium(IV) chlorides were reported to act as potent antihelminic [26] and immunomodulator agents [27].

In view of above interesting features shown and our continued interest in chemistry of tellurium(IV) complexes, we developed a series of organyltellurium(IV) complexes with 1-(((4-hydroxyphenyl)imino)methyl)naphthalen-2-ol ligand. The synthesized ligand (H4AP) and organyltellurium(IV) complexes were characterized with the help of conductance

measurement, elemental analyses, mass spectrometry, UV-Vis, ^{13}C NMR, ^{1}H NMR, FT-IR spectroscopy and further screened for antimicrobial and antioxidant activities.

EXPERIMENTAL

All the chemicals were acquired from Aldrich Chemicals Co., USA and used as received. Solvents used were procured from CDH, India and distilled according to reported procedure before use [28]. Tellurium compounds were prepared according to the literature methods.

Physical measurements: Elemental analysis (C, H, N) were estimated using a CHN analyzer. The FT-IR spectra were carried out (KBr and polyethylene disc) in the mid-IR and far-IR region on Nicolet iS-50 FT-IR spectrophotometer. The absorption spectra were measured on a Shimadzu UV-3600 Plus instrument in the wavelength range 200-800 nm. ^{13}C NMR and ^{1}H NMR measurements were recorded on Bruker Advance III 400 MHz FT NMR spectrometer using DMSO-d_6 as solvent and TMS as standard. Mass spectrum of the compounds were recorded on SCIEX Triple TOF 5600 mass spectrometer. Melting point were recorded using capillary technique and are uncorrected. Molar Conductance was measured using MICROSIL conductivity meter.

Computational calculation: Density function theory based computational calculations of all the synthesized compounds have been successfully achieved through Orca software using DFT method with def2-SVP basis sets. Resultant optimized geometries of the compounds were visualized using Avogadro 4.0 software.

Antioxidant activity: The antioxidant activity of Schiff base and its organyltellurium(IV) complexes were evaluated on the basis of DPPH radical scavenging activity. For this, different concentration of the synthesized compounds were added in DPPH solution and then incubated in dark for 30 min. Ascorbic acid was used as standard. Absorbance of each solution was recorded at 517 nm. The radical scavenging activity was evaluated using the following equation:

$$\text{Inhibition } (\%) = \frac{A - B}{A} \times 100$$

where A is absorbance of ascorbic acid and B is the absorbance of sample. The inhibitory concentration (IC_{50}) values were calculated from the plot of % inhibition *versus* concentration. The DPPH radical scavenging activity is inversely proportional to the IC_{50} value of sample that means lower the value of IC_{50} higher is the antioxidant activity.

Antimicrobial activity: The antimicrobial activity of ligand and its organyltellurium(IV) complexes (**1a-f**) were studied using Broth microdilution method and determined in terms of the MIC (minimum inhibitory concentration) values. The synthesized compounds were screened against two Gram-positive bacterial species, two Gram-negative bacterial species and three fungal species. Ampicillin and greseofulvin were used as the standard drugs, respectively for the antibacterial and antifungal activities. The MIC value of the compounds were determined using microdilution technique with two-fold set of serial dilution screening using concentration of 1000, 500 and 250 µg/mL for the initial screening and concentrations of 200, 100, 50, 25, 12.5 and 6.25 µg/mL for the secondary screening. The cultures of bacteria and fungi were incubated at 37 ºC for overnight.

Molecular docking: The pdb files of the proteins *C. albicans* (PDB ID: 3dra) and *E. coli* (PDB ID: 3t88) were obtained from the RCSB protein data bank. The 3D structures of the synthesized ligand 1-(((4-hydroxyphenyl)imino)methyl)naphthalen-2-ol was drawn in Avogadro software and then converted into pdb format using Pymol software. The molecular docking of the ligand into receptor proteins were performed using MGL tools and Autodock Vina. The results obtained from docking were visualized using the Pymol software.

Synthesis of 1-(((4-hydroxyphenyl)imino)methyl)-naphthalen-2-ol (H4AP): Ligand 1-(((4-hydroxyphenyl)-imino)methyl)naphthalen-2-ol was prepared by refluxing equimolar quantities (20 mM) of 2-hydroxy-1-naphthaldehyde (3.443 g, 25 mL) with 4-aminophenol (2.182 g, 25 mL) in ethanol. The resulting solution was stirred for 4 h under reflux (60 ºC) and kept aside at room temperature for overnight [29]. The precipitate obtained was filtered, washed twice with cold ethanol and dried in vacuum condition (**Scheme-I**). Colour: orange. Yield: 94%. *m.w.*: 263.31 g/mol. m.p.: 210-212 ºC. ^{1}H NMR (DMSO-d_6, δ ppm): 14.19 (s, 1H, naphthyl -OH), 10.86 (s, 1H, phenyl -OH), 8.40 (s, 1H, -CH=N-), 8.03-6.85 (m, 10H, Ar-H). ^{13}C NMR (DMSO-d_6, δ (ppm): 108.96 (C_1), 158.18 (C_2), 119.50 (C_3), 130.40 (C_4), 129.11 (C_5), 127.01 (C_6), 122.80 (C_7), 125.80 (C_8), 118.54 (C_9), 131.00 (C_{10}), 165.04 (C_{11}), 143.41 (C_{12}), 121.45 ($C_{13,17}$), 115.80 ($C_{14.16}$), 155.13 (C_{15}). UV-Vis (λ_{max}, nm): 203,238, 360, 424. Anal. calcd. (found) % for $C_{17}H_{13}NO_2$: C, 77.55 (77.58); H, 4.96 (4.93); N, 5.32 (5.29). FT-IR (KBr, ν_{max}, cm^{-1}): 3464 (O-H), 3066 (Ar C-H), 2925 (C-H), 1624 (C=N), 1240 (C-O). MS: *m/z* (264.10).

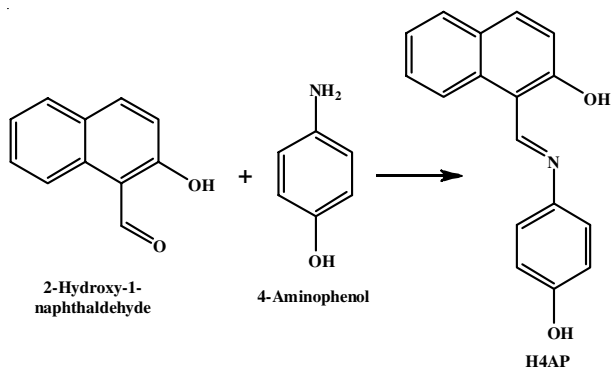

Scheme-I: Synthesis of ligand H4AP

Synthesis of organyltellurium(IV) chlorides ($RTeCl_3$/R_2TeCl_2): Different organyltellurium(IV) chlorides ($RTeCl_3$ and R_2TeCl_2) such as 3-methyl-4-hydroxyphenyl tellurium(IV) trichlorides, 4-hydroxyphenyl tellurium(IV) trichlorides, 4-methoxyphenyl tellurium(IV) trichlorides, *bis*-(3-methyl-4-hydroxyphenyl)tellurium(IV) dichloride, *bis*-(4-hydroxyphenyl)tellurium(IV) dichloride, *bis*-(4-methoxyphenyl) tellurium(IV) dichloride, were synthesized by the reaction of $TeCl_4$ with the different arenes *i.e. o*-cresol/anisole/phenol according to the analogous reported methods [30-38].

$$RH + TeCl_4 \longrightarrow RTeCl_3$$

$$2RH + TeCl_4 \longrightarrow R_2TeCl_2$$

where R-H = anisole, *o*-cresol and phenol.

Synthesis of complexes ($RTeCl_2$·H4AP and R_2TeCl·H4AP): To organyltellurium(IV) chloride in methanol, Schiff base ligand H4AP dissolved in methanol was added slowly while stirring. The solution was heated under reflux for 5 h. The resultant solution volume was reduced to one third and evaporated to dryness. The solid precipitates obtained were recrystallized with petroleum ether and chloroform and dried in vacuum condition (**Scheme-II**).

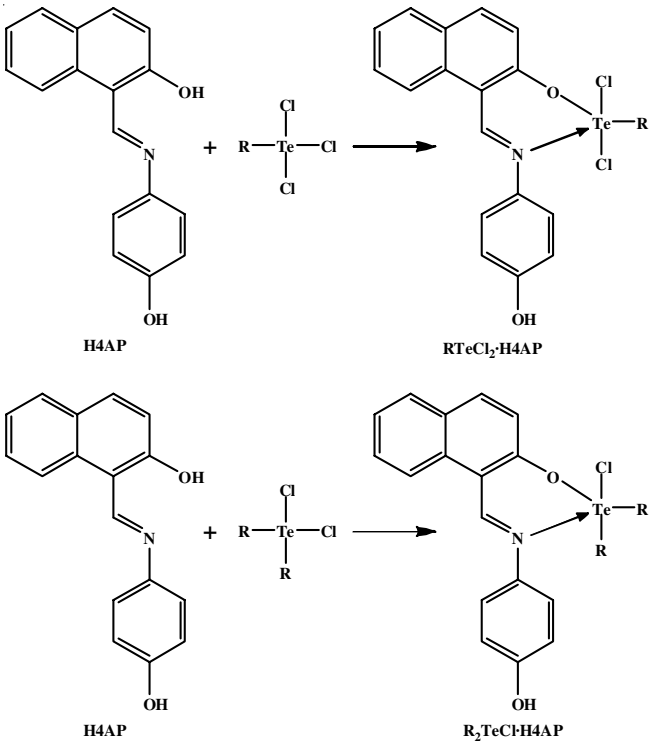

Scheme-II: Synthesis of $RTeCl_2$·H4AP and R_2TeCl·H4AP

$RTeCl_2$·H4AP (4-methoxyphenyl) (1a): Colour: brown. Yield: 82%. m.w.: 567.91 g/mol. m.p.: 120-122 ºC. ^{1}H NMR (DMSO-d_6, δ ppm): 10.81 (s, 1H, phenyl -OH), 8.48 (s, 1H, -CH=N-), 8.00-6.87 (m, 14H, Ar-H), 3.69 (s, 3H, -OCH_3). ^{13}C NMR (DMSO-d_6, δ ppm): 109.70 (C_1), 160.81 (C_2), 119.50 (C_3), 130.40 (C_4), 129.11 (C_5), 127.01 (C_6), 122.80 (C_7), 125.80 (C_8), 118.60 (C_9), 131.09 (C_{10}), 169.43 (C_{11}), 143.60 (C_{12}), 121.50 ($C_{13,17}$), 115.81 ($C_{14.16}$), 155.13 (C_{15}), 114.30 (C_{18}), 133.40 ($C_{19,23}$), 123.50 ($C_{20,22}$), 153.60 (C_{21}), 55.70 (C_{24}). UV-Vis (λ_{max}, nm): 205,242, 394, 485. Anal. calcd. (found) % for $C_{24}H_{19}Cl_2NO_3Te$: C, 50.74 (50.56); H, 3.39 (3.05); N, 2.41 (2.27); Te, 22.47 (21.43); Cl, 12.51 (11.75). FT-IR (KBr, ν_{max}, cm^{-1}): 3400 (O-H), 3185 (Ar C-H), 2970 (C-H), 1605 (C=N), 1223 (C-O), 517 (Te-N), 295 (Te-O). MS: *m/z* (567.88).

$RTeCl_2$·H4AP (4-hydroxyphenyl) (1b): Colour: brown. Yield: 87%. m.w.: 553.88 g/mol. m.p.: 110-112 ºC. ^{1}H NMR (DMSO-d_6, δ ppm): 10.86 (s, 2H, phenyl -OH), 8.99 (s, 1H, -CH=N-), 8.17-6.98 (m, 14H, Ar-H). ^{13}C NMR (DMSO-d_6, δ ppm): 108.99 (C_1), 161.09 (C_2), 119.90 (C_3), 130.50 (C_4), 129.10 (C_5), 127.10 (C_6), 122.90 (C_7), 125.78 (C_8), 118.62 (C_9), 131.15 (C_{10}), 171.40 (C_{11}), 143.67 (C_{12}), 121.60 ($C_{13,17}$), 115.90 ($C_{14.16}$), 155.41 (C_{15}), 114.70 (C_{18}), 133.84 ($C_{19,23}$), 114.79 ($C_{20,22}$), 156.51 (C_{21}). UV-Vis (λ_{max}, nm): 220,257, 403, 480. Anal. calcd. (found) % for $C_{23}H_{17}Cl_2NO_3Te$: C, 49.87 (49.03); H, 3.07 (2.84); N, 2.53 (2.19); Te, 23.04 (22.09); Cl, 12.82 (12.17). FT-IR (KBr, ν_{max}, cm^{-1}): 3460 (O-H), 3067 (Ar C-H), 2990 (C-H), 1594 (C=N), 1216 (C-O), 505 (Te-N), 289 (Te-O). MS: *m/z* (553.80).

$RTeCl_2$·H4AP (3-methyl-4-hydroxyphenyl) (1c): Colour: yellowish brown. Yield: 75%. m.w.: 567.92 g/mol. m.p.: 120-122 ºC. ^{1}H NMR (DMSO-d_6, δ ppm): 10.84 (s, 2H, phenyl -OH), 9.16 (s, 1H, -CH=N-), 8.15-6.91 (m, 13H, Ar-H), 2.20 (s, 3H, -CH_3). ^{13}C NMR (DMSO-d_6, δ (ppm): 109.78 (C_1), 162.98 (C_2), 119.60 (C_3), 130.45 (C_4), 129.11 (C_5), 127.04 (C_6), 122.85 (C_7), 125.80 (C_8), 118.62 (C_9), 131.11 (C_{10}), 169.99 (C_{11}), 143.89 (C_{12}), 121.65 ($C_{13,17}$), 115.92 ($C_{14.16}$), 155.98 (C_{15}), 114.60 (C_{18}), 133.80 ($C_{19,23}$), 126.00 (C_{20}), 155.01 (C_{21}), 115.80 (C_{22}), 21.38 (C_{24}). UV-Vis (λ_{max}, nm): 203,251, 385, 479. Anal. calcd. (found) % for $C_{24}H_{19}Cl_2NO_3Te$: C, 50.76 (50.15); H, 3.35 (3.07); N, 2.47 (2.59); Te, 22.47 (21.11); Cl, 12.50 (12.09). FT-IR (KBr, ν_{max}, cm^{-1}): 3442 (O-H), 3110 (Ar C-H), 3010 (C-H), 1610 (C=N), 1213 (C-O), 511 (Te-N), 293 (Te-O). MS: *m/z* (567.95).

R_2TeCl·H4AP (4-methoxyphenyl) (1d): Colour: brown. Yield: 80%. m.w.: 639.61 g/mol. m.p.: 140-142 ºC. ^{1}H NMR (DMSO-d_6, δ ppm): 10.86 (s, 1H, phenyl -OH), 8.51 (s, 1H, -CH=N-), 8.08-6.87 (m, 18H, Ar-H), 3.71 (s, 6H, -OCH_3). ^{13}C NMR (DMSO-d_6, δ (ppm): 109.19 (C_1), 160.91 (C_2), 119.50 (C_3), 130.40 (C_4), 129.11 (C_5), 127.01 (C_6), 122.80 (C_7), 125.80 (C_8), 118.60 (C_9), 131.09 (C_{10}), 169.90 (C_{11}), 143.60 (C_{12}), 121.50 ($C_{13,17}$), 115.81 ($C_{14.16}$), 155.15 (C_{15}), 114.30 ($C_{18,25}$), 133.49 ($C_{19,23,26,30}$), 123.40 ($C_{20,22,27,29}$), 153.65 ($C_{21,28}$), 55.60 ($C_{24,31}$). UV-Vis (λ_{max}, nm): 218,254, 389, 486. Anal. calcd. (found) % for $C_{31}H_{26}ClNO_4Te$: C, 58.21 (58.09); H, 4.08 (3.90); N, 2.19 (2.01); Te, 19.94 (19.18); Cl, 5.56 (5.01). FT-IR (KBr, ν_{max}, cm^{-1}): 3480 (O-H), 3091 (Ar C-H), 2997 (C-H), 1597 (C=N), 1226 (C-O), 516 (Te-N), 285 (Te-O). MS: *m/z* (639.68).

R_2TeCl·H4AP (4-hydroxyphenyl) (1e): Colour: orange. Yield: 87%. m.w.: 611.54 g/mol. m.p.: 174-176 ºC. ^{1}H NMR (DMSO-d_6, δ ppm): 10.89 (s, 3H, phenyl -OH), 9.00 (s, 1H, -CH=N-), 8.12-6.91 (m, 18H, Ar-H). ^{13}C NMR (DMSO-d_6, δ ppm): 109.78 (C_1), 161.42 (C_2), 119.90 (C_3), 130.50 (C_4), 129.10 (C_5), 127.10 (C_6), 122.90 (C_7), 125.78 (C_8), 118.62 (C_9), 131.15 (C_{10}), 171.80 (C_{11}), 143.67 (C_{12}), 121.60 ($C_{13,17}$), 115.90 ($C_{14,16}$), 155.40 (C_{15}), 114.70 ($C_{18,24}$), 133.80 ($C_{19,23,25,29}$), 114.79 ($C_{20,22,26,28}$), 156.50 ($C_{21,27}$). UV-Vis (λ_{max}, nm): 217, 255, 401, 479. Anal. calcd. (found) % for $C_{29}H_{22}ClNO_4Te$: C, 56.96 (56.18); H, 3.63 (3.17); N, 2.29 (2.03); Te, 20.87 (20.11); Cl, 5.80 (5.17). FT-IR (KBr, ν_{max}, cm^{-1}): 3400 (O-H), 3086 (Ar C-H), 2979 (C-H), 1594 (C=N), 1217 (C-O), 509 (Te-N), 288 (Te-O). MS: *m/z* (611.48).

R_2TeCl·H4AP (3-methyl-4-hydroxyphenyl) (1f): Colour: green. Yield: 83%. m.w.: 639.61 g/mol. m.p.: 141-143 ºC. ^{1}H NMR (DMSO-d_6, δ (ppm): 10.84 (s, 3H, phenyl -OH), 9.21 (s, 1H, -CH=N-), 8.16-6.91 (m, 16H, Ar-H), 2.19 (s, 6H, -CH_3). ^{13}C NMR (DMSO-d_6, δ ppm): 109.78 (C_1), 162.97 (C_2), 119.60

(C_3), 130.45 (C_4), 129.11 (C_5), 127.04 (C_6), 122.85 (C_7), 125.80 (C_8), 118.62 (C_9), 131.11 (C_{10}), 170.21 (C_{11}), 143.89 (C_{12}), 121.65 ($C_{13,17}$), 115.92 ($C_{14.16}$), 155.70 (C_{15}), 114.60 ($C_{18,25}$), 133.86 ($C_{19,23,26,30}$), 126.10 ($C_{20,27}$), 155.00 ($C_{21,28}$), 115.80 ($C_{22,29}$), 21.30 ($C_{24,31}$). UV-Vis (λ_{max}, nm): 210,240, 387, 484. Anal. calcd. (found) % for $C_{31}H_{26}ClNO_4Te$: C, 58.25 (57.79); H, 4.06 (3.91); N, 2.18 (2.02); Te, 19.95 (19.81); Cl, 5.56 (5.03). FT-IR (KBr, ν_{max}, cm^{-1}): 3380 (O-H), 3062 (Ar C-H), 2960 (C-H), 1598 (C=N), 1217 (C-O), 517 (Te-N), 295 (Te-O). MS: *m/z* (639.81).

RESULTS AND DISCUSSION

The newly synthesized Schiff base (H4AP) and its organyltellurium(IV) complexes were coloured, stable under normal laboratory conditions and are soluble in solvents like chloroform, ethanol, DMSO, *etc*.

Conductance studies: The molar conductance (Λ_m) of 10^{-3} M of their solutions were measured at 25 ºC and reported in Table-1. The resulting values lies in the range 46.47-11.72 S cm^2 mol^{-1} indicating their weak electrolyte [39,40] nature in DMSO solvent, conductance values were possibly due to the ionization into $(RTeCl{\cdot}H4AP)^+/(R_2Te{\cdot}H4AP)^+$ and Cl^- in DMSO solvent.

TABLE-1
MOLAR CONDUCTANCE OF
ORGANYLTELLURIUM(IV) COMPLEXES

Compound	Molar conductance (S cm^2 mol^{-1})
1a	41.00
1b	46.47
1c	46.07
1d	40.88
1e	40.06
1f	11.72

IR spectra: Key IR absorption bands of ligand (H4AP) and organyltellurium(IV) complexes (**1a-f**) are represented in Table-2. Comparison of FT-IR spectra of complexes with ligand (H4AP) was done to determine structures and its ligation behaviour. The characteristic stretching vibration peaks at 3432, 3066, 2925 and 1240 cm^{-1} are ascribed to O-H, aromatic C-H, aliphatic C-H and C-O bond of ligand [40], respectively. The bands at 1514 and 1541 cm^{-1} correspond to the symmetric and asymmetric stretching vibration of C=C bonds. The absorption band at 1624 cm^{-1} ascribed to the C=N stretching vibration [20] of ligand shifted to 1607-1596 cm^{-1} in complexes indicating that imine group is attached to metal centre through nitrogen. Intense peak at 1240 cm^{-1} corresponding to C-O stretching in ligand, shifted to lower wavenumber indicating naphthyl hydroxyl oxygen of ligand is involved in coordination with tellurium. Appearance of new absorption bands in the region 298-281 cm^{-1} and 525-507 cm^{-1} ascribed to ν(Te-O) [39,41] and ν(Te-N) [41-43] confirms the coordination of naphthyl oxygen and imine nitrogen with tellurium. The in-plane and out of plane bending vibration of C-H bond were observed at 1020 cm^{-1} and 833 cm^{-1}.

Mass spectra: The mass spectra of ligand H4AP (Fig. 1a) exhibited a molecular ion peak (M^+) at *m/z* 264.10 (theoretical 263.29). The result is consistent with the suggested molecular formula of the ligand [44]. The mass spectra for the complexes **1a**, **1b**, **1c**, **1d**, **1e** and **1f** show *m/z* value at 567.88, 553.80, 567.95, 639.68, 611.48 and 639.81, respectively (Fig. 1b). The measured *m/z* values are completely compatible with the theoretical ones confirming that each complex keep its mononuclear structure, with the 1:1 of ligand to organyltellurium(IV) chlorides.

UV-Vis spectra: The electronic absorption spectra of ligand (H4AP) and its organyltellurium(IV) complexes were measured using $BaSO_4$ as a solid phase. The spectral data is summarized in Table-3. Electronic spectra of ligand [29,44] exhibited bands at 203, 248 nm assignable to π-π* transitions. The band seen at 360 nm is ascribed to n-π* transition of the imine group. The band at 424 nm in ligand is due to charge transfer transition within the ligand molecule. For complexes, the shifts of the characteristic bands toward longer wavelength comparable to the Schiff base ligand (H4AP), confirms the complexes formation (Fig. 2).

^{1}H NMR spectra: The ^{1}H NMR spectral data of Schiff base (H4AP) and organyltellurium(IV) complexes (**1a-f**) are presented in Table-4. In the proton NMR spectrum, the ligand exhibits a singlet peak at δ 8.40 ppm for the imine (CH=N) proton [29], shifted to δ 8.48-9.21 ppm in complexes indicating involvement of imine nitrogen in complexation. The singlet peak at δ 14.19 ppm corresponding to hydroxyl proton [44] of 2-hydroxynaphthaldehyde moiety of ligand is absent in spectrum of complexes suggesting deprotonated oxygen is involved in coordination. The phenolic proton of aminophenol moiety appearing as singlet peak at δ 10.86 ppm remain appreciably same on their position in spectrum of complexes. In the spectrum of ligand, aromatic protons appeared in the range δ 6.85-8.03 ppm slightly shifted downfield in the complexes due to decreased electron density after complexation.

^{13}C NMR spectra: The ^{13}C NMR spectrum data of Schiff base (H4AP) and organyltellurium(IV) complexes are shown in Table-5. In the ^{13}C NMR spectrum of Schiff base and its

TABLE-2
IMPORTANT INFRARED ABSORPTION BANDS (cm^{-1}) OF LIGAND (H4AP) AND Te(IV) COMPLEXES

Compound	O-H	C-H (aromatic)	C-H	C=N	C-O	Te-N	Te-O
H4AP	3432s	3066s	2925s	1624s	1240s	–	–
1a	3400w	3085m	2970s	1605s	1223s	517s	295s
1b	3460w	3067m	2990s	1599s	1216s	505m	289m
1c	3442s	3110s	2998m	1596s	1213s	511m	293m
1d	3480s	3091s	2997w	1607s	1226s	516s	285s
1e	3400w	3086w	2979s	1604s	1217s	509s	288s
1f	3380m	3062w	2960s	1606s	1217s	517m	295s

s = sharp, m = medium, mb = medium broad, sh = shoulder and w = weak

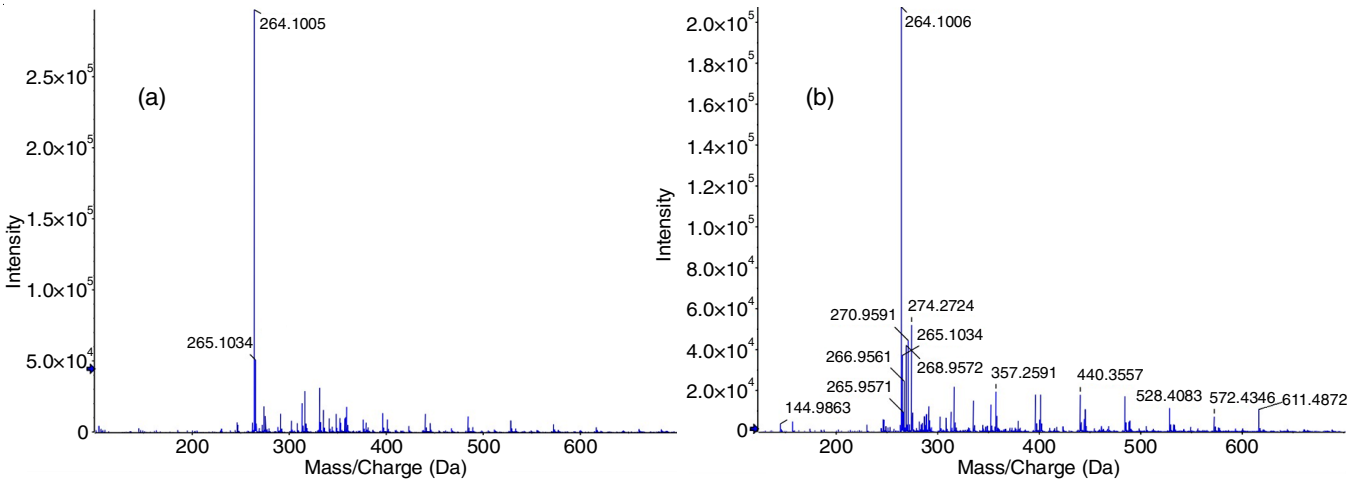

Fig. 1. Mass spectrum of (a) ligand (H4AP) and (b) $R_2TeCl{\cdot}H4AP$ (**1e**)

TABLE-3
ELECTRONIC SPECTRAL DATA OF LIGAND (H4AP) AND COMPLEXES

Compound	λ_{max}, nm (cm^{-1})			
	π–π*		n–π*	Charge transfer
H4AP	203 (49261)	248 (42016)	360 (27777)	424 (23584)
1a	205 (48780)	242 (41322)	394 (25380)	485 (20618)
1b	220 (45454)	257 (38910)	403 (24814)	480 (20833)
1c	203 (49261)	251 (39841)	385 (25974)	479 (20876)
1d	218 (45871)	254 (39370)	389 (25706)	486 (20576)
1e	217 (46082)	255 (39216)	401 (24937)	479 (20876)
1f	210 (47619)	240 (41666)	387 (25840)	484 (20661)

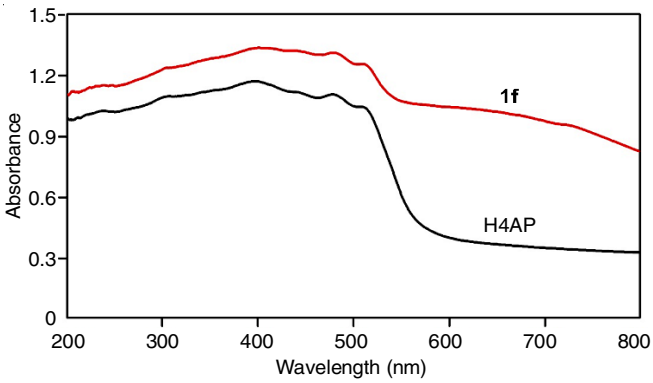

Fig. 2. UV-visible spectrum of ligand (H4AP) and complex $R_2TeCl{\cdot}H4AP$ (**1f**)

synthesized complexes, aromatic carbon [29,44,45] signals were observed in the range δ 108.96-156.50 ppm. Peaks shown by ligand at δ 165.04 ppm and 158.18 ppm corresponding to imine carbon (C_{11}), aromatic carbon attached to -OH group of naphthaldehyde part of ligand (C_2) were shifted to downfield in the range δ 169.43-172.00 ppm, δ 160.00-163.00 ppm supporting the coordination of imine-N and naphthyl-O to tellurium(IV) ion in the complexes. No appreciable change was found in the peak observed at δ 155.13 ppm assigned to aromatic carbon attached with the -OH group of aminophenol moiety, indicating its non-participation in complexation.

Geometry optimization: Molecular geometry optimization of Schiff base and its organyltellurium(IV) complexes (**1a** and **1e**) was done with zero numerical constraints using Avogadro 4.0 program with Orca visualization software. The resultant optimized geometries of the ligand H4AP and the complexes **1a** and **1e** are given in Fig. 3. From the optimized structures, it has been seen that the ligand is fully planar while the complexes have a twisted structure in its optimized form. In ligand (Table-6), the C=N (imine) and C-O (naphthyl) bond

TABLE-4
^{1}H NMR SPECTRAL STUDIES OF LIGAND (H4AP) AND Te(IV) COMPLEXES

Compound	Chemical Shift, δ ppm (in DMSO-d_6)				
	OH (naphthyl)	OH (phenol)	CH=N	Aromatic protons	CH_3/-OCH_3**
H4AP	14.19 (s, 1H)	10.86 (s, 1H)	8.40 (s, 1H)	8.03-6.85 (m, 10H)	–
1a	–	10.81 (s, 1H)	8.48 (s, 1H)	8.00-6.87 (m, 14H)	3.69 (s, 3H)**
1b	–	10.86 (s, 2H)	8.99 (s, 1H)	8.17-6.98 (m, 14H)	–
1c	–	10.84 (s, 2H)	9.16 (s, 1H)	8.15-6.91 (m, 13H)	2.20 (s, 3H)
1d	–	10.86 (s, 1H)	8.51 (s, 1H)	8.08-6.87 (m, 18H)	3.71 (s, 6H)**
1e	–	10.89 (s, 3H)	9.00 (s, 1H)	8.12-6.91 (m, 18H)	–
1f	–	10.84 (s, 3H)	9.21 (s, 1H)	8.16-6.91 (m, 16H)	2.19 (s, 6H)

TABLE-5
^{13}C NMR SPECTRAL STUDIES OF LIGAND (H4AP) AND Te(IV) COMPLEXES

Compound	Chemical Shift, δ ppm (in DMSO-d_6)				
	C=N	C-OH (naphthyl)	C-OH (aminophenol)	Aromatic carbons	Aliphatic carbons (CH_3/OCH_3**)
H4AP	165.04 (C_{11})	158.18 (C_2)	155.13 (C_{15})	108.96 (C_1), 119.50 (C_3), 130.40 (C_4), 129.11 (C_5), 127.01 (C_6), 122.80 (C_7), 125.80 (C_8), 118.54 (C_9), 131.00 (C_{10}), 143.41 (C_{12}), 121.45 ($C_{13,17}$), 115.80 ($C_{14.16}$)	–
1a	169.43 (C_{11})	160.81 (C_2)	155.13 (C_{15})	109.70 (C_1), 119.50 (C_3), 130.40 (C_4), 129.11 (C_5), 127.01 (C_6), 122.80 (C_7), 125.80 (C_8), 118.60 (C_9), 131.09 (C_{10}), 143.60 (C_{12}), 121.50 ($C_{13,17}$), 115.81 ($C_{14.16}$), 114.30 (C_{18}), 133.40 ($C_{19,23}$), 123.50 ($C_{20,22}$), 153.60 (C_{21})	55.70 (C_{24})**
1b	171.40 (C_{11})	161.09 (C_2)	155.41 (C_{15})	108.99 (C_1), 119.90 (C_3), 130.50 (C_4), 129.10 (C_5), 127.10 (C_6), 122.90 (C_7), 125.78 (C_8), 118.62 (C_9), 131.15 (C_{10}), 143.67 (C_{12}), 121.60 ($C_{13,17}$), 115.90 ($C_{14.16}$), 114.70 (C_{18}), 133.84 ($C_{19,23}$), 114.79 ($C_{20,22}$), 156.51 (C_{21})	–
1c	169.99 (C_{11})	162.98 (C_2)	155.98 (C_{15})	109.78 (C_1), 119.60 (C_3), 130.45 (C_4), 129.11 (C_5), 127.04 (C_6), 122.85 (C_7), 125.80 (C_8), 118.62 (C_9), 131.11 (C_{10}), 143.89 (C_{12}), 121.65 ($C_{13,17}$), 115.92 ($C_{14.16}$), 114.60 (C_{18}), 133.80 ($C_{19,23}$), 126.00 (C_{20}), 155.01 (C_{21}), 115.80 (C_{22})	21.38 (C_{24})
1d	169.90 (C_{11})	160.91 (C_2)	155.15 (C_{15})	109.19 (C_1), 119.50 (C_3), 130.40 (C_4), 129.11 (C_5), 127.01 (C_6), 122.80 (C_7), 125.80 (C_8), 118.60 (C_9), 131.09 (C_{10}), 143.60 (C_{12}), 121.50 ($C_{13,17}$), 115.81 ($C_{14.16}$), 114.30 ($C_{18.25}$), 133.49 ($C_{19,23,26,30}$), 123.40 ($C_{20,22,27,29}$), 153.65 ($C_{21,28}$)	55.60 ($C_{24,31}$)**
1e	171.80 (C_{11})	161.42 (C_2)	155.40 (C_{15})	109.78 (C_1), 119.90 (C_3), 130.50 (C_4), 129.10 (C_5), 127.10 (C_6), 122.90 (C_7), 125.78 (C_8), 118.62 (C_9), 131.15 (C_{10}), 143.67 (C_{12}), 121.60 ($C_{13,17}$), 115.90 ($C_{14.16}$), 114.70 ($C_{18.24}$), 133.80 ($C_{19,23,25,29}$), 114.79 ($C_{20,22,26,28}$), 156.50 ($C_{21,27}$)	–
1f	170.21 (C_{11})	162.97 (C_2)	155.70 (C_{15})	109.78 (C_1), 119.60 (C_3), 130.45 (C_4), 129.11 (C_5), 127.04 (C_6), 122.85 (C_7), 125.80 (C_8), 118.62 (C_9), 131.11 (C_{10}), 143.89 (C_{12}), 121.65 ($C_{13,17}$), 115.92 ($C_{14.16}$), 114.60 ($C_{18.25}$), 133.86 ($C_{19,23,26,30}$), 126.10 ($C_{20,27}$), 155.00 ($C_{21,28}$), 115.80 ($C_{22,29}$)	21.30 ($C_{24,31}$)

**Due to -OCH_3 moiety

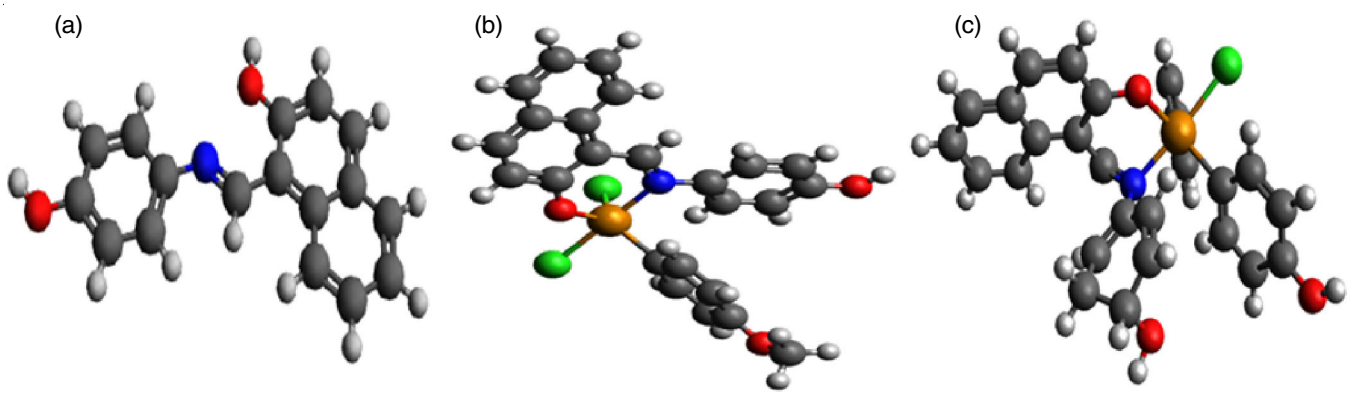

Fig. 3. Optimized structure of (a) ligand H4AP; (b) complex **1a**; (c) complex **1e**; Ball colour code: grey-C; red-O; blue-N; green-Cl; yellow-Te; white-H

length were found to be of 1.290 Å and 1.335 Å, respectively and in the complexes bond lengths were found in the range 1.295-1.305 Å and 1.339-1.373 Å, elongation in bond lengths indicates their involvement in complexation. The theoretically calculated bond angles of the complexes (Table-7) predicts distorted square pyramidal geometry around the tellurium ion comprehensively supporting the purposed structures of the complexes.

Frontier molecular orbital (FMO) analysis: The frontier molecular orbitals termed as quantum orbitals [46-49] includes

TABLE-6
CALCULATED BOND LENGTH (Å) DATA OF LIGAND H4AP, COMPLEXES **1a** AND **1e**

Compound	ν(C=N)	ν(C-O) (naphthyl)	ν(C-O) (aminophenol)	ν(Te-N)	ν(Te-O)
H4AP	1.290	1.335	1.348	–	–
1a	1.305	1.339	1.348	2.091	1.970
1e	1.295	1.373	1.348	2.073	2.038

TABLE-7
THEORETICAL CALCULATED BOND ANGLES FOR THE COMPLEX $R_2TeCl{\cdot}H4AP$ (**1a**)

Atom connectivity	Bond angles (°)	Atom connectivity	Bond angles (°)
N-Te-O	92.3967	N-Te-Cl	179.1652
O-Te-Cl	117.6256	N-Te-C	91.1663
O-Te-Cl	87.8197	Cl-Te-Cl	88.9785
O-Te-C	116.4420	Cl-Te-C	125.7967
N-Te-Cl	90.2070	Cl-Te-C	89.4586

lowest unoccupied molecular orbital (LUMO) and highest occupied molecular orbital (HOMO). Fig. 4 displays the both LUMO and HOMO images of the ligand and complex **1a** and **1e**. For ligand, the HOMO energy was found at -5.079 eV while the LUMO energy is at -2.629 eV, with a 2.45 eV energy gap. For complexes **1a** and **1e**, HOMO energies were found at -3.895 eV and -3.431 eV, and the LUMO energies were at -1.900 eV and -1.431 eV, respectively. The HOMO-LUMO energy gap for the complex **1a** and **1e** is 1.995 eV and 2.000 eV *i.e.* energy gap is decreased indicating the successful complexation of Schiff base ligand with tellurium ion. Different quantum parameters [49] evaluated from the HOMO and LUMO energy levels are tabulated in Table-8. From the optimized structure of ligand, HOMO and LUMO is mainly located on whole pi-bond system. In complexes **1a** and **1e**, electron density of HOMO is mainly concentrated on tellurium ion with involvement of heteroatoms of ligand moiety, while LUMO is totally ligand centric.

Antioxidant activity: In this study, 2,2-diphenyl-1-picryl-hydrazyl radical scavenging activity was used to assess antioxidant activity of the synthesized compounds. The percentage inhibition for ligand (**H4AP**) and its organyltellurium(IV) complexes (**1a-f**) are shown in Fig. 5. The IC_{50} values of the synthesized compounds were calculated and compared with the standard ascorbic acid (Table-9). The results revealed that the complexes have higher antioxidant activity than the Schiff base except complex **2f**. Complex **2a** (IC_{50} = 52.14 µg/mL) has the highest antioxidant activity as compared to the ligand (IC_{50} = 235.60 µg/mL) and ascorbic acid (IC_{50} = 73.71 µg/mL) making it as good antioxidant agent.

TABLE-8
THEORETICAL CALCULATED QUANTUM CHEMICAL PARAMETERS OF THE LIGAND H4AP AND COMPLEXES **1a** AND **1e**

Quantum chemical parameters	H4AP	**1a**	**1e**
E_{HOMO} (eV)	-5.079	-3.895	-3.431
E_{LUMO} (eV)	-2.629	-1.900	-1.431
ΔE (eV)	2.450	1.995	2.000
I (eV)	5.079	3.895	3.431
A (eV)	2.629	1.900	1.431
χ (eV)	3.854	2.898	2.431
η (eV)	1.225	0.998	1.000
σ (eV^{-1})	0.816	1.002	1.000
S (eV^{-1})	0.408	0.501	0.500
ω (eV)	6.060	4.207	4.727
Pi (eV)	-3.854	-2.898	-2.431
ΔN_{max}	3.146	2.903	2.431

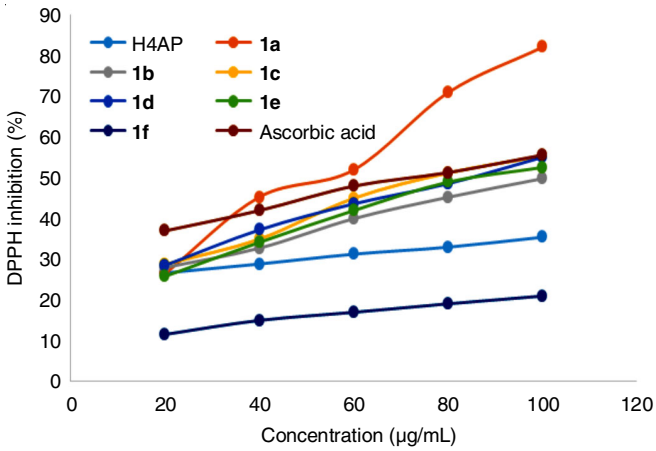

Fig. 5. DPPH radical scavenging activity of the ligand (H4AP) and its complexes (**1a-f**)

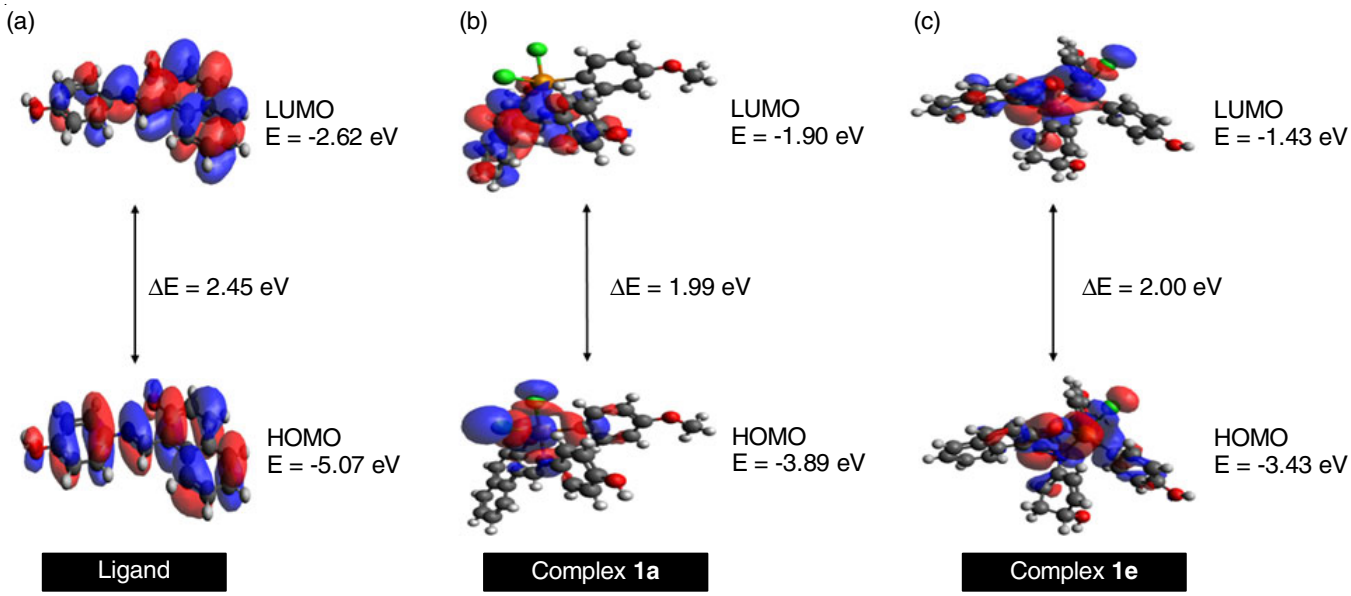

Fig. 4. HOMO-LUMO gap energies of (a) ligand; (b) complex **1a**; (c) complex **1e**

TABLE-9
ANTIOXIDANT DATA OF THE LIGAND H4AP AND ITS CORRESPONDING COMPLEXES (**1a-f**)

Compound	IC_{50} (μg/mL)
H4AP	235.6
1a	52.14
1b	98.48
1c	79.88
1d	83.06
1e	87.16
1f	349.29
Ascorbic acid	73.71

Antibacterial activity: The synthesized ligand (H4AP) and its organyltellurium(IV) complexes were examined against few microorganisms such as *P. aeruginosa, S. pyogenes*, *E. coli* and *S. aureus* to assess their capability as antibacterial agent. The minimum inhibition concentration (MIC) in mg/mL for the ligand and complexes against the growth of bacterial species. The results (Table-10) show that the synthesized organyltellurium(IV) complexes have higher activity than the Schiff base (**H4AP**) against the similar bacterial species. The enhanced growth inhibition activity of the complexes is due to their strong chelating ability. All the organyltellurium(IV) complexes were found to be most effective against *S. aureus* and *S. pyogenes* bacterial specie and least active against *E. coli*. Among all the complexes, complex **1a** ($RTeCl_2$·H4AP, R = 4-methoxyphenyl) was found to be most potent having lowest MIC value against all the tested bacterial species, whereas complex **1d** (R_2TeCl·H4AP, R = 4-methoxyphenyl) exhibits good activity against *P. aeruginosa*, *S. aureus, S. pyogenes* and lower activity against *E. coli*.

TABLE-10
MINIMUM INHIBITORY CONCENTRATION OF THE LIGAND (H4AP) AND COMPLEXES (**1a-f**) AGAINST THE GROWTH OF BACTERIAL SPECIES (mg/mL)

Compound	*S. aureus*	*S. pyogenes*	*E. coli*	*P. aeruginosa*
H4AP	1.0	0.5	0.5	0.5
1a	0.1	0.0625	0.0625	0.05
1b	0.5	0.5	0.5	0.25
1c	0.5	0.2	0.25	0.5
1d	0.2	0.1	0.125	0.0625
1e	0.125	0.1	0.5	0.5
1f	0.2	0.0625	0.125	0.125
Ampicillin	0.25	0.1	0.1	0.1

Antifungal activity: The antifungal activity of synthesized Schiff base (**H4AP**) and organyltellurium(IV) complexes (**1a-f**) were investigated against *A. clavatus*, *A. niger* and *C. albicans* fungal species. The results (Table-11) revealed that complexes shows the better antifungal activity than the synthesized ligand (**H4AP**) against *A. niger* and *C. albicans* fungal species and lower activity against *A. clavatus.* Among the complexes, most of them show promising activity against *C. albicans* fungal specie and lower activity against *A. niger* and *A. clavatus* fungal species except complex **1f** (R_2TeCl·H4AP, R = 3-methyl-4-hydroxyphenyl), which show excellent activity against all the fungal species as compared to standard drug greseofulvin.

TABLE-11
MINIMUM INHIBITORY CONCENTRATION OF THE LIGAND (H4AP) AND COMPLEXES (**1a-f**) AGAINST THE GROWTH OF FUNGAL SPECIES (mg/mL)

Compound	*C. albicans*	*A. niger*	*A. clavatus*
H4AP	0.5	1.0	1.0
1a	0.2	0.5	1.0
1b	1.0	0.5	1.0
1c	0.1	0.1	1.0
1d	0.1	0.5	1.0
1e	0.5	1.0	0.5
1f	0.2	0.1	0.1
Greseofulvin	0.5	0.1	0.1

Molecular docking: Molecular docking studies of 1-(((4-hydroxyphenyl)imino)methyl)naphthalen-2-ol with the different proteins: *E. coli* and *C. albicans* was carried out to discover the binding modes [50,51] present between the protein and the ligand. Resulted docked conformation of ligand with receptor proteins are displayed in Fig. 6, which confirms that the ligand is embedded into the deep cavity of the receptor proteins. The molecular docking results revealed that different type of interaction are present between the Schiff base and amino acid residues of proteins. For receptor *C. albicans*, three hydrogen bonding interaction was found between the residues His145 and Arg160 and the ligand with the bond length 2.2 Å, 2.5 Å and 2.3 Å. For *E. coli*, ligand forms four hydrogen bonds with Gly242 (bond length 1.9 Å), Ala238 (bond length 1.8 Å), Asp239 (bond length 2.5 Å) and Arg173 (bond length 2.8 Å) amino acid residues. Apart from these hydrogen bonding interactions, few hydrophobic non polar interactions are also present between the Schiff base and amino acid residues of proteins. The relative binding energy of docked structures was found to be -8.3 Kcal/mol (*C. albicans*) and -8.4 Kcal/mol (*E. coli*), respectively.

Conclusion

In this work, the synthesis of six new organyltellurium(IV) complexes of 1-(((4-hydroxyphenyl)imino)methyl)naphthalen-2-ol Schiff base (H4AP). Based on elemental analyses, molar conductance, mass, FT-IR, UV-visible, ^{1}H NMR and ^{13}C NMR spectroscopies, ligand was found to act in bidentate manner and bound to metal ion through imine nitrogen and hydroxyl oxygen atom of naphthalene moiety. Spectroscopic studies predicted distorted square pyramidal geometry around the tellurium ion for the complexes (**1a-f**). The geometry of the ligand and Te(IV) complexes were fully optimized at def2-SVP level of theory and results show that the obtained geometry of the tellurium complexes were similar to that concluded by spectroscopic analysis. Result of molecular docking simulation support the bioactivity results and therefore Schiff base can be considered as potent antimicrobial agent. However, the synthesized organyltellurium(IV) complexes showed better antimicrobial activity than the corresponding ligand.

ACKNOWLEDGEMENTS

The authors thanks Maharshi Dayanand University, Rohtak, India for CHN analysis, UV and FT-IR studies. One of the

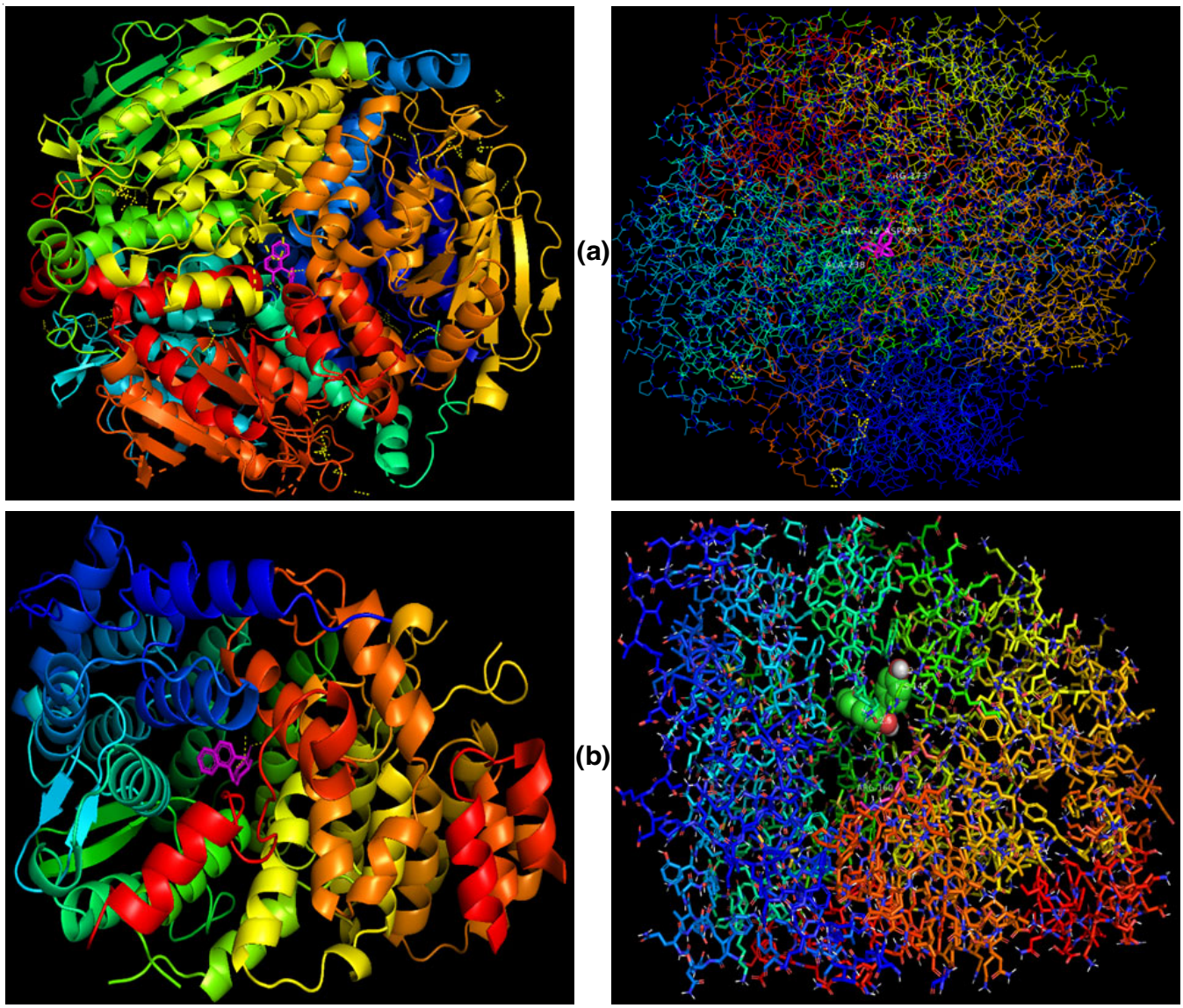

Fig. 6. 3D plot of interaction of (a) ligand H4AP with *E. coli* (3t88) and (b) ligand H4AP with *C. albicans* (3dra)

authors, Mahak Dalal thanks UGC, New Delhi, India for the financial support. Thanks are also due to G.J. University, Hisar, India for mass and NMR studies; and Microcare Laboratory and Tuberculosis Research Centre, Surat, India for the antimicrobial studies.

CONFLICT OF INTEREST

The authors declare that there is no conflict of interests regarding the publication of this article.

REFERENCES

1. E. Raczuk, B. Dmochowska, J. Samaszko-Fiertek and J. Madaj, *Molecules*, **27**, 787 (2022); https://doi.org/10.3390/molecules27030787
2. A. Prakash, B.K. Singh, N. Bhojak and D. Adhikari, *Spectrochim. Acta A Mol. Biomol. Spectrosc.*, **76**, 356 (2010); https://doi.org/10.1016/j.saa.2010.03.019
3. P. Rathelot, P. Vanelle, M. Gasquet, F. Delmas, M.P. Crozet, P. Timon-David and J. Maldonado, *Eur. J. Med. Chem.*, **30**, 503 (1995); https://doi.org/10.1016/0223-5234(96)88261-4
4. S. Smitha, S.N. Pandeya, J.P. Stables and S. Ganapathy, *Sci. Pharm.*, **76**, 621 (2008); https://doi.org/10.3797/scipharm.0806-14
5. M. Sirajuddin, N. Uddin, S. Ali and M.N. Tahir, *Spectrochim. Acta A Mol. Biomol. Spectrosc.*, **116**, 111 (2013); https://doi.org/10.1016/j.saa.2013.06.096
6. R. Selvarani, S. Balasubramaniyan, K. Rajasekar, M. Thairiyaraja and R. Meenakshi, *Asian J. Chem.*, **33**, 1222 (2021); https://doi.org/10.14233/ajchem.2021.23150
7. W. Al Zoubi, A. A. S. Al-Hamdani and M. Kaseem, *Appl. Organomet. Chem.*, **30**, 810 (2016); https://doi.org/10.1002/aoc.3506
8. Neelofar, N. Ali, A. Khan, S. Amir, N.A. Khan and M. Bilal, *Bull. Chem. Soc. Ethiop.*, **31**, 445 (2017); https://doi.org/10.4314/bcse.v31i3.8
9. C. Festus, A.C. Ekennia, A.A. Osowole, L.O. Olasunkanmi, D.C. Onwadiwe and O.T. Ujam, *Res. Chem. Intermed.*, **44**, 5857 (2018); https://doi.org/10.1007/s11164-018-3460-7
10. A.C. Ekennia, A.A. Osowole, L.O. Olasunkanmi, D.C. Onwadiwe and E.E. Ebenso, *Res. Chem. Intermed.*, **43**, 3787 (2017); https://doi.org/10.1007/s11164-016-2841-z
11. H.L. Singh, J.B. Singh and S. Bhanuka, *Res. Chem. Intermed.*, **42**, 997 (2016); https://doi.org/10.1007/s11164-015-2069-3

12. A.F. Shoair, A.R. El-Shobaky and H.R. Abo-Yassin, *J. Mol. Liq.*, **211**, 217 (2015); https://doi.org/10.1016/j.molliq.2015.07.001
13. X. Zhao, C. Li, S. Zeng and W. Hu, *Eur. J. Med. Chem.*, **46**, 52 (2011); https://doi.org/10.1016/j.ejmech.2010.10.010
14. M.J. Hearn, M.H. Cynamon, M.F. Chen, R. Coppins, J. Davis, H.J.-O. Kang, A. Noble, B. Tu-Sekine, M.S. Terrot, D. Trombino, M. Thai, E.R. Webster and R. Wilson, *Eur. J. Med. Chem.*, **44**, 4169 (2009); https://doi.org/10.1016/j.ejmech.2009.05.009
15. L. Antonov, W.M.F. Fabian, D. Nedeltcheva and F.S. Kamounah, *J. Chem. Soc., Perkin Trans. 2*, **6**, 1173 (2000); https://doi.org/10.1039/b000798f
16. J. Devi, M. Yadav, A. Kumar and A. Kumar, *Chem. Pap.*, **72**, 2479 (2018); https://doi.org/10.1007/s11696-018-0480-0
17. S. Ranjith, P. Sugumar, G. Rajagopal, M. Udayakumar and M.N. Ponnuswamy, *J. Mol. Struct.*, **1065-1066**, 21 (2014); https://doi.org/10.1016/j.molstruc.2014.02.025
18. N. Bouzayani, S. Marque, B. Djelassi, Y. Kacem, J. Marrot and B. Ben Hassine, *New J. Chem.*, **42**, 6389 (2018); https://doi.org/10.1039/C7NJ04597B
19. M.M. Rahman, T.A. Sheikh, R.M. El-Shishtawy, M.N. Arshad, F.A.M. Al-Zahrani and A.M. Asiri, *RSC Adv.*, **8**, 19754 (2018); https://doi.org/10.1039/C8RA01827H
20. T. Kiran, V.G. Prasanth, M.M. Balamurali, C.S. Vasavi, P. Munusami, K.I. Sathiyanarayanan and M. Pathak, *Inorg. Chim. Acta*, **433**, 26 (2015); https://doi.org/10.1016/j.ica.2015.04.033
21. N. Uddin, F. Rashid, S.Y. Tirmizi, I. Ahmad, S. Zaib, M. Zubair, P.L. Diaconescu, M.N. Tahir, J. Iqbal and A. Haider, *J. Biomol. Struct. Dynam.*, **38**, 3246 (2019); https://doi.org/10.1080/07391102.2019.1654924
22. Z. Abbasi, M. Salehi, A. Khaleghian and M. Kubicki, *J. Mol. Struct.*, **1173**, 213 (2018); https://doi.org/10.1016/j.molstruc.2018.06.104
23. I. Guest and J. Uetrecht, *Expt. Hematol.*, **29**, 123 (2001).
24. T.A. Alorini, A.N. Al-Hakimi, S. El-Sayed Saeed, E.H.L. Alhamzi and A.E.A.E. Albadri, *Arab. J. Chem.*, **15**, 103559 (2022); https://doi.org/10.1016/j.arabjc.2021.103559
25. S. Jain, M. Rana, R. Sultana, R. Mehandi and Rahisuddin, *Polycycl. Arom. Comp.*, **56**, 1040 (2022); https://doi.org/10.1080/10406638.2022.2117210
26. A.P. Ordyntseva, I.D. Sivovolsva, G.M. Abakarov and E.I. Sadekova, *Pharm. Chem. J.*, **22**, 703 (1988); https://doi.org/10.1007/BF00763667
27. R.L. Cunha, I.E. Gouvea and L. Juliano, *An. Acad. Bras. Cienc.*, **81**, 393 (2009); https://doi.org/10.1590/S0001-37652009000300006
28. A.I. Vogel, Practical Organic Chemistry, Including Qualitative Organic Analysis, Longmans, Green and Co. London, New York, Toranto, Ed. 3, Vol. 1188, p. 300 (1956).
29. S. Chahmana, S. Keraghel, F. Benghanem, R. Ruiz-Rosas, A. Ourari and E. Morallon, *Int. J. Electrochem. Sci.*, **13**, 175 (2018); https://doi.org/10.20964/2018.01.27
30. B.L. Khandelwal, K. Kumar and F.J. Berry, *Inorg. Chim. Acta*, **47**, 135 (1981); https://doi.org/10.1016/S0020-1693(00)89319-6
31. B.L. Khandelwal, K. Kumar and K. Reina, *Synth. React. Inorg. Met. Chem.*, **11**, 65 (1981); https://doi.org/10.1080/00945718108059276
32. J. Bergman, *Tetrahedron*, **28**, 3323 (1972); https://doi.org/10.1016/S0040-4020(01)93674-9
33. M.V. Garad, *Polyhedron*, **4**, 1353 (1985); https://doi.org/10.1016/S0277-5387(00)86963-6
34. W.J. Geary, *Coord. Chem. Rev.*, **7**, 81 (1971); https://doi.org/10.1016/S0010-8545(00)80009-0
35. F.J. Berry, E.H. Kustan, M. Roshani and B.C. Smith, *J. Organomet. Chem.*, **99**, 115 (1975); https://doi.org/10.1016/S0022-328X(00)86367-6
36. G.T. Morgan and H.D.K. Drew, *J. Chem. Soc. Trans.*, **127**, 2307 (1925); https://doi.org/10.1039/CT9252702307
37. G.T. Morgan and R.E. Kellet, *J. Chem. Soc.*, **129**, 1080 (1926); https://doi.org/10.1039/JR9262901080
38. N. Petragnani and H.A. Stefani, Tellurium in Organic Synthesis, Academic Press: London, Ed.: 2 (2007).
39. N.S. Biradar, T.M. Aminabhavi, C.M. Patil and W.E. Rudzinski, *Inorg. Chim. Acta*, **78**, 47 (1983); https://doi.org/10.1016/S0020-1693(00)86487-7
40. B. Uba, M.G. Liman and M. Sikiru, *Sch. J. App. Med. Sci.*, **5(10B)**, 3940 (2017).
41. I. Haiduc, R.B. King and M.G. Newton, *Chem. Rev.*, **94**, 301 (1994); https://doi.org/10.1021/cr00026a002
42. D.J. Birdsall, J. Novosad, A.M.Z. Slawin and J.D. Woollins, *J. Chem. Soc. Dalton Trans.*, 435 (2000); https://doi.org/10.1039/A907336A
43. Y.D. Kulkarni, S. Srivastava, S.H.R. Abdi and M. Athar, *Synth. React. Inorg. Met.-Org. Chem.*, **15**, 1043 (1985); https://doi.org/10.1080/00945718508060634
44. I. Kaya and A. Bilici, *J. Macrmol. Sci. Part A*, **43**, 719 (2006); https://doi.org/10.1080/10601320600602688
45. A.I. Demehin, M.A. Oladipo and B. Semire, *Eclét. Quím.*, **45**, 18 (2020); https://doi.org/10.26850/1678-4618eqj.v45.1.2020.p18-43
46. T. Abbaz, A. Bendjeddon and D. Villemin, *Int. J. Adv. Sci. Eng. Technol.*, **5**, 5150 (2018).
47. Sh.M. Morgan, A.Z. El-Sonbati and M.A. El-Mogazy, *Appl. Organomet. Chem.*, **32**, e4264 (2018); https://doi.org/10.1002/aoc.4264
48. N.F. Ugwu, C.J.O. Anarado, C.U. Ibeji, O.C. Okpareke, C.J. Ezeorah, O.D. Okagu, A.C. Ekennia, F. Cömert, I. Babahan, B. Coban and O.T. Ujam, *ChemistrySelect*, **4**, 11206 (2019); https://doi.org/10.1002/slct.201902870
49. S. Abbas, H.H. Nasir, S. Zaib, S. Ali, T. Mahmood, K. Ayub, M.N. Tahir and J. Iqbal, *J. Mol. Struct.*, **1156**, 193 (2018); https://doi.org/10.1016/j.molstruc.2017.11.086
50. W.H. Mahmoud, N.E. Mahmoud and G.G. Mohamed, *J. Organomet. Chem.*, **848**, 288 (2017); https://doi.org/10.1016/j.jorganchem.2017.08.001
51. W.H. Mahmoud, G.G. Mohamed and A.M. Refat, *Appl. Organomet. Chem.*, **31**, e3753 (2017); https://doi.org/10.1002/aoc.3753